FULLY-DIFFERENTIAL SINGLE RESONATOR FM/WHOLE ANGLE GYROSCOPE USING CW/CCW MODE SEPARATOR

Takashiro Tsukamoto and Shuji Tanaka
Department of Robotics, Tohoku University, Sendai, Japan

ABSTRACT

This paper reports a fully-differential frequency modulated (FM) gyroscope where superposed clockwise (CW) and counter clockwise (CCW) modes are independently controlled on a single resonator. A CW/CCW mode separator was implemented with a mode-matched ring resonator, and FM gyroscope operation with excellent linearity between applied angular rate and frequency difference was demonstrated. The scale factor was as high as 0.724, and measured almost zero temperature coefficient including ±26 ppm uncertainty without any compensation. Whole angle mode operation was also demonstrated using the same system and excellent linear relationship between applied rotation angle and measured angle was observed.

BACKGROUND

A frequency modulated (FM) gyroscope has unique advantages such as low temperature sensitivity of scale factor [1, 2] and wide bandwidth. The FM gyroscope uses a 2-dimensional mode-matched resonator. Two eigenmodes are degenerated when angular rate input is zero. An applied angular rate, Ω, resolves the degeneracy, generating two eigenmodes: clockwise (CW) and counter-clockwise (CCW) rotation modes. The eigenfrequencies are given as

$$\omega_{\mathrm{cw}} = 2\pi f_{\mathrm{cw}} = \omega_0(T) + k\Omega \tag{1}$$

$$\omega_{\mathrm{ccw}} = 2\pi f_{\mathrm{ccw}} = \omega_0(T) - k\Omega, \tag{2}$$

where $f_0 (= \omega_0/2\pi)$, k and T are a natural frequency of the resonator, a scale factor and temperature, respectively.

The natural frequency, $\omega_0(T)$, has a temperature sensitivity, which causes the bias error. However, this temperature-induced frequency change can be cancelled out by measuring a frequency difference, $\Delta\omega = \omega_{\mathrm{ccw}} - \omega_{\mathrm{cw}}$. This principle was confirmed by spectral-analyzing ring-down vibration of a high Q MEMS resonator [1]. More practical FM gyroscopes were recently reported, but two modes were excited on two resonators [3], or shared a single resonator with time division drive [2, 4]. The two resonator system requires a pair of highly mode-matched resonators, which raises fabrication difficulty, and temperature difference between two resonators induces bias error. On the other hand, the time division drive system has a limited bandwidth of measurement.

In this paper, we propose a fully-differential FM gyroscope which independently but simultaneously controls both CW and CCW modes on a single resonator. Compared with the previous works, the proposed system works with only one resonator, and the continuous excitation of both modes solves the bandwidth problem. In addition, the system can be used as a whole angle gyroscope, which detects the rotation angle rather than the angular rate.

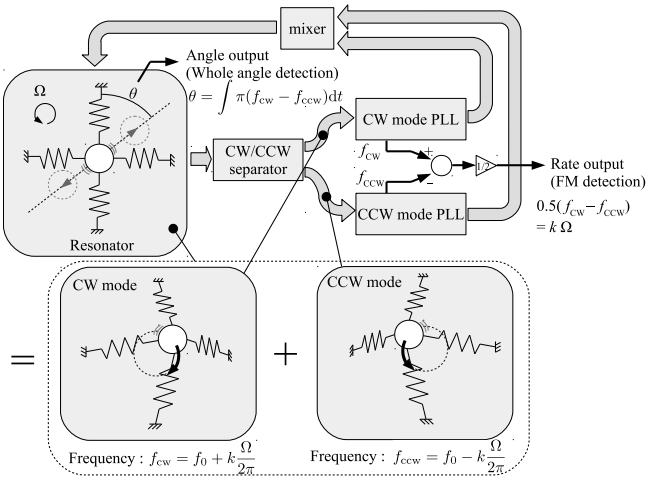

Figure 1: Schematic of FM/whole angle gyroscope system using CW/CCW mode separator

WORKING PRINCIPLE OF FM/WHOLE ANGLE GYROSCOPE

Figure 1 shows the principle and schematic diagram of a proposed FM/whole angle gyroscope. Two eigenmodes (CW and CCW modes) are simultaneously excited on a single resonator. By using a CW/CCW mode separator, these modes can be separated and independently controlled using each phase locked loop (PLL). The linear combination of these two modes results in a linear oscillation as

$$\begin{aligned}\begin{bmatrix} x \\ y \end{bmatrix} &= \begin{bmatrix} 1 \\ i \end{bmatrix} \mathrm{e}^{i\phi_{\mathrm{cw}}} + \begin{bmatrix} 1 \\ -i \end{bmatrix} \mathrm{e}^{i\phi_{\mathrm{ccw}}} \\ &= 2\begin{bmatrix} \cos\left(k\int \Omega \mathrm{d}t\right) \\ -\sin\left(k\int \Omega \mathrm{d}t\right) \end{bmatrix} \mathrm{e}^{i\int \omega_0 \mathrm{d}t} \\ &= 2\begin{bmatrix} \cos(\theta) \\ \sin(\theta) \end{bmatrix} \mathrm{e}^{i\int \omega_0 \mathrm{d}t}, \end{aligned} \tag{3}$$

where the phase of CW and CCW mode can be expressed as

$$\phi_{\mathrm{cw}} = \int \omega_{\mathrm{cw}} \mathrm{d}t = \int \omega_0 \mathrm{d}t + k\int \Omega \mathrm{d}t \tag{4}$$

$$\phi_{\mathrm{ccw}} = \int \omega_{\mathrm{ccw}} \mathrm{d}t = \int \omega_0 \mathrm{d}t - k\int \Omega \mathrm{d}t, \tag{5}$$

respectively. Thus, the oscillation direction, θ, changes with the integration of angular rate, $\Theta = \int \Omega \mathrm{d}t$, like the Foucault pendulum, which means the system can work not only as a rate gyroscope but also as a whole angle gyroscope.

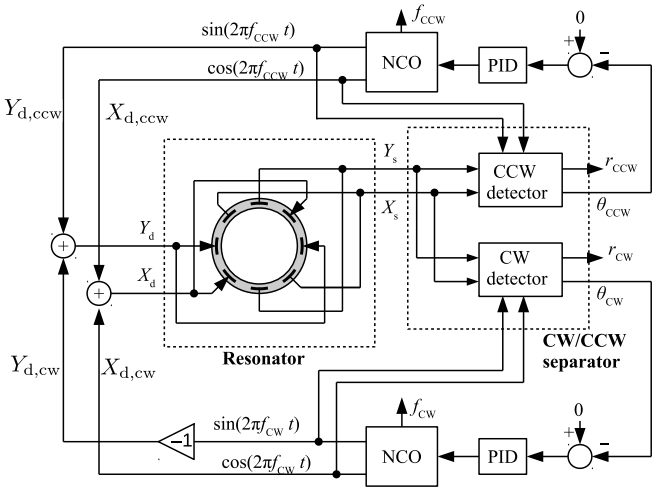

Figure 2: Control diagram of gyroscope.

Figure 2 shows the detailed description of the control system diagram. The CW/CCW mode separator consists of CW and CCW detectors. The signal processing procedure of which is based on synchronous detection as illustrated in Fig. 3. The phase of each mode, θ_{cw} or θ_{ccw}, is kept at each resonance point using the standard PLL technology. A numerical controlled oscillator (NCO) generates both X and Y drive signals with a phase difference of $\pm 90^\circ$ to excite each of CW or CCW mode.

The angular rate can be obtained by the frequency difference between two modes as

$$\Omega = \frac{\omega_{\rm cw} - \omega_{\rm ccw}}{2k}, \tag{6}$$

and the rotation angle can be obtained as

$$\Theta = \frac{1}{k}\tan^{-1}\left(\frac{A_x}{A_y}\right), \tag{7}$$

where A_x and A_y are X and Y oscillation amplitudes, respectively.

EXPERIMENT

Experimental setup

Figure 4 shows an experimental setup. We used a highly mode-matched ring resonator (SGH03, Silicon Sensing Systems, UK). The resonance frequency was 14 kHz and the mode mismatch was as small as 2 ppm. The resonator was fixed on a rate table. The temperature of which was controlled by a feedback controlled Peltier element. Two digital lock-in amplifiers (UHF-LI, Zurich Instruments Ltd., Switzerland) were used for both CW and CCW PLLs. Resonator output was measured by an oscilloscope and the oscillation direction was calculated according to Eq. (7).

FM mode operation

Figure 5 shows the measured X and Y amplitudes of the resonator. When only the CW or CCW mode PLL was activated, the resonator showed circular trajectory with $\pm 90^\circ$

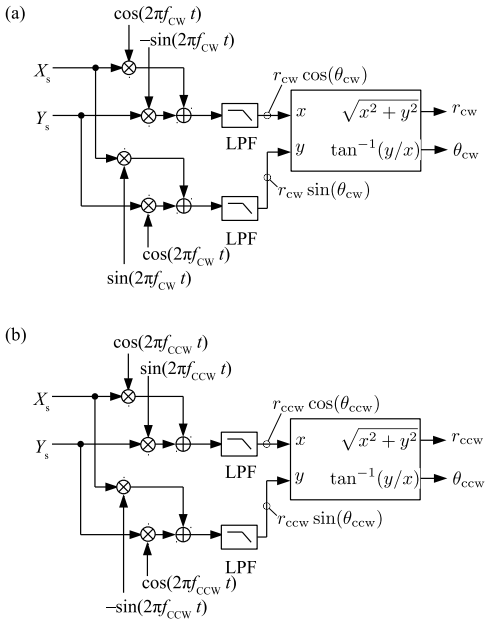

Figure 3: Signal processing procedure of (a) CW and (b) CCW detectors.

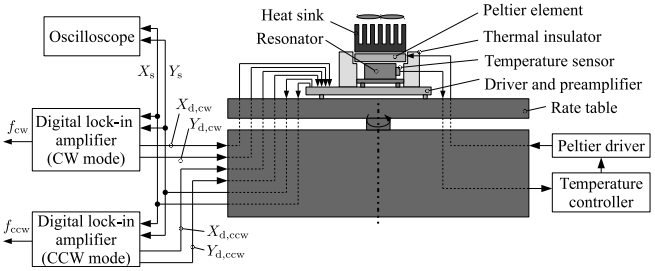

Figure 4: Experimental setup.

phase difference between X and Y oscillation (Fig. 5(a)-(d)). When both CW and CCW mode PLL were activated, the resulting oscillation was linear shape as explained by Eq. (3), i.e. the phase difference between X and Y was 0° or 180° (Fig. 5(e), (f)).

Figure 6 shows the measured frequencies of both CW and CCW modes at 25°C and 75°C. Both CW and CCW mode frequencies were almost identical when no rotation applied ($\Omega = 0$). When positive angular rate ($\Omega > 0$) was applied, CW and CCW resonant frequencies respectively increased and decreased by the same amount, and the negative angular rate induced the opposite frequency change. Due to the temperature dependency of silicon, the resonance frequency changed with temperature, but the frequency difference between CW and CCW had no temperature dependency. Figure 7 shows the relationship between the frequency difference ($\Delta\omega = \omega_{\rm cw} - \omega_{\rm ccw} = 2\pi(f_{\rm cw} - f_{\rm ccw})$) and applied angular rate (Ω). The frequency difference linearly changed according to the applied angular rate with a proportional factor (i.e. the scale factor) of 0.724.

Figure 8 shows the scale factor under various temperature conditions. The measured temperature

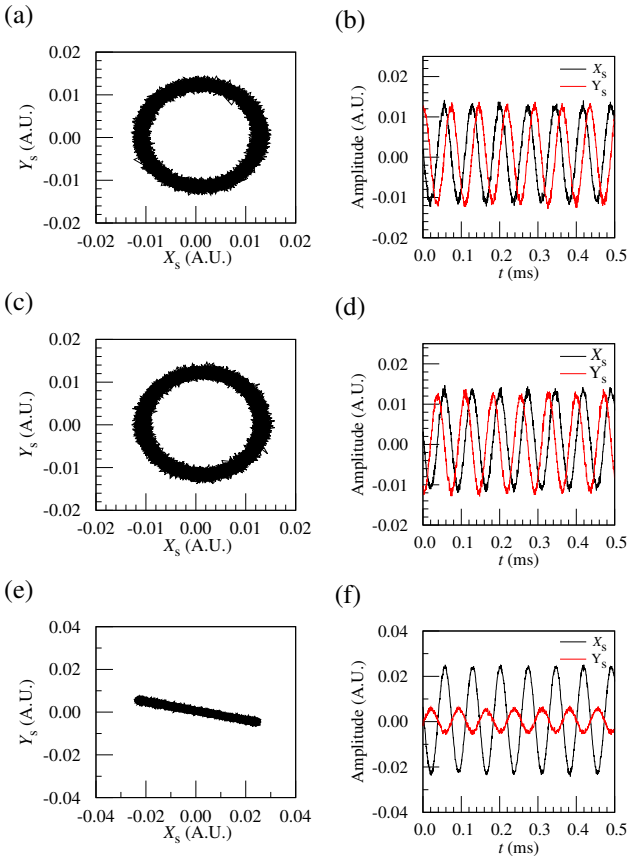

Figure 5: Oscillation amplitude of resonator driven by (a, b) only CW mode PLL, (c, d) only CCW mode PLL and (e, f) both CW and CCW mode PLLs, simultaneously.

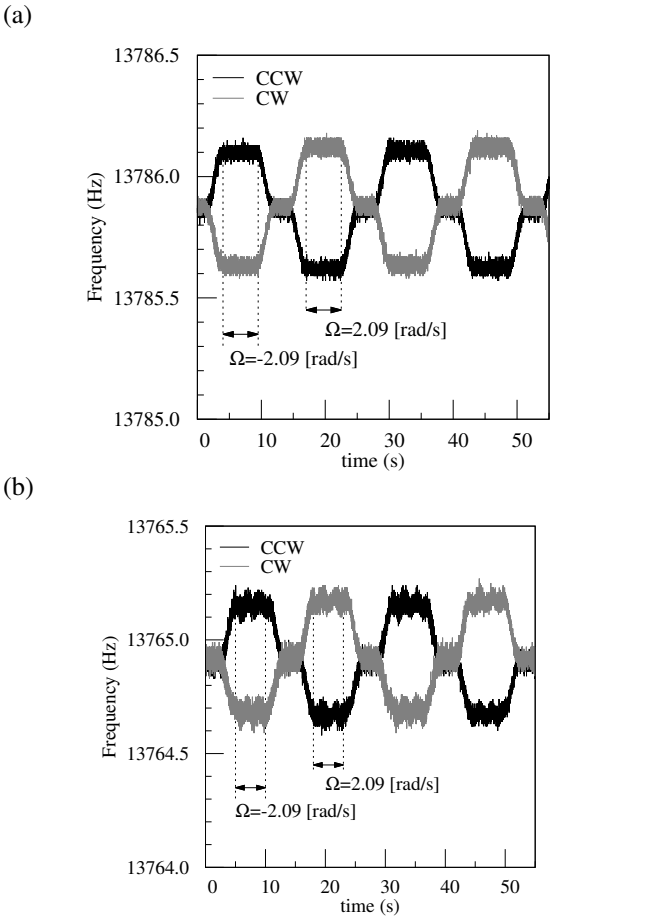

Figure 6: CW and CCW resonant frequencies at (a) 25°C and (b) 75°C.

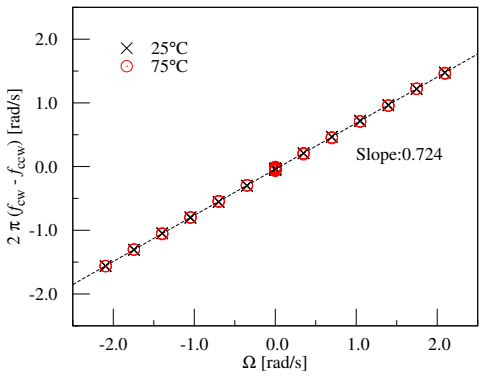

Figure 7: FM output (frequency difference) under different input rate.

coefficient was almost zero including ±26 ppm uncertainty without any compensation.

Whole angle mode operation

Figure 9 shows the X and Y amplitudes of the resonator with the angular rate of 1.74 rad/s. As shown in Fig. 9 (b)-(e), X and Y oscillations were in-phase (phase difference was 0° or 180°), which means the linear oscillation was stably excited by the superposed CW and CCW modes. The sinusoidal change of the amplitude (Fig. 9 (a)) indicates that the oscillation direction linearly changed with time, and that the system worked as the whole angle gyroscope.

Figure 10 shows the time history of oscillation direction, $\theta = \tan^{-1}(A_y/A_x)$, under the angular rate of ±1.74 rad/s. An excellent linear relationship between oscillation direction, θ, and applied rotation, $\Theta = \int \Omega dt$, was observed. By linear regression fitting, the rate of direction change is obtained as $\frac{d\theta}{dt} = 1.26$ [rad/s]. Thus, the scale factor of whole angle mode is obtained as $k = 0.724$, which is the same value with the FM mode result.

Compared with the previous reported whole angle gyroscopes, our method has the following advantages. The linearity is excellent even when no compensation technique is applied [5, 6]. The PLL does not lose lock state at specific oscillation directions [6]. The oscillation can be excited continuously [7].

CONCLUSION

A single resonator FM/whole angle gyroscope system using a CW/CCW mode separator was developed. The FM mode operation showed excellent linearity between measured

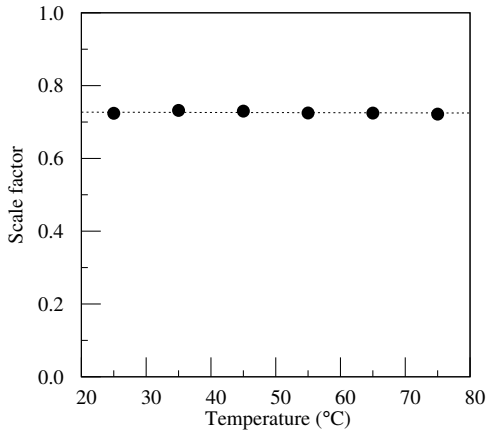

Figure 8: Temperature dependency of scale factor.

frequency difference and applied angular rate. The scale factor was 0.724 with almost zero temperature coefficient with ±26 ppm measurement uncertainty. The whole angle mode operation showed excellent linearity between measured oscillation direction an applied rotation angle with the same scale factor of 0.724. The proposed control system is promising for a navigation grade MEMS gyroscope.

REFERENCES

[1] S. Zotov, A. Trusov and A. Shkel, "High-Range Angular Rate Sensor Based on Mechanical Frequency Modulation," *J. Microelectromech. Syst*, **21**, pp. 398–405, 2012.

[2] B. Eminoglu, Y. C. Yeh, I. I. Izyumin, I. Nacita, M. Wireman, A. Reinelt and B. E. Boser, "Comparison of long-term stability of AM versus FM gyroscopes," in *Proc. IEEE MEMS 2016*, Jan 2016, pp. 954–957.

[3] M. Kline, Y. Yeh, B. Eminoglu, H. Najar, M. Daneman, D. Horsley and B. Boser, "Quadrature FM gyroscope," in *Proc. IEEE MEMS 2013*, Jan 2013, pp. 604–608.

[4] I. I. Izyumin, M. H. Kline, Y. C. Yeh, B. Eminoglu, C. H. Ahn, V. A. Hong, Y. Yang, E. J. Ng, T. W. Kenny and B. E. Boser, "A 7ppm, 6°/hr frequency-output MEMS gyroscope," in *Proc. IEEE MEMS 2015*, Jan 2015, pp. 33–36.

[5] J. A. Gregory, J. Cho and K. Najafi, "Novel mismatch compensation methods for rate-integrating gyroscopes," in *Proc. Position Location and Navigation Symposium (PLANS), 2012 IEEE/ION*, April 2012, pp. 252–258.

[6] J. K. Woo, J. Y. Cho, C. Boyd and K. Najafi, "Whole-angle-mode micromachined fused-silica birdbath resonator gyroscope (WA-BRG)," in *Proc. IEEE MEMS 2014*, Jan 2014, pp. 20–23.

[7] I. P. Prikhodko, S. A. Zotov, A. A. Trusov and A. M. Shkel, "Foucault pendulum on a chip: Rate integrating silicon MEMS gyroscope," *Sens. Actuators, A*, **177**, pp. 67–78, 2012.

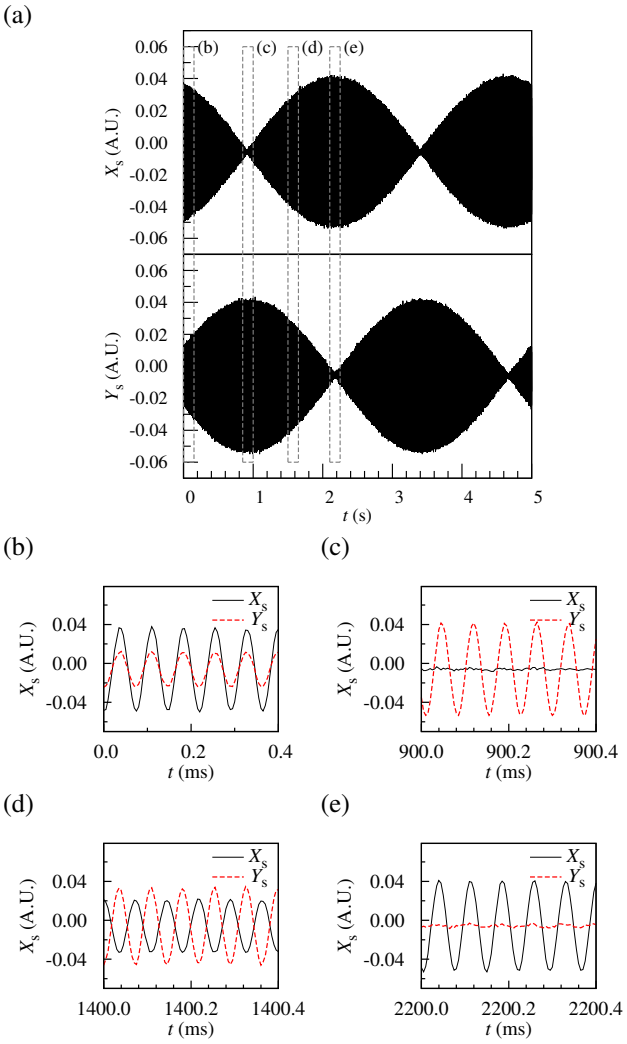

Figure 9: Oscillation amplitudes of both X and Y axis.

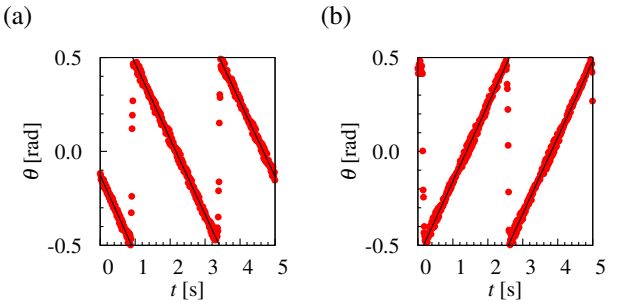

Figure 10: Measured oscillation direction, θ, under the angular rate of (a) 1.74 rad/s and (b) −1.74 rad/s.

CONTACT

T. Tsukamoto, tel: +81-22-795-6937; t_tsuka@mems.mech.tohoku.ac.jp